Low-Frequency Raman Spectroscopy of n-Alcohols. LAM Vibration and Crystal Structure

ARTICLE *in* THE JOURNAL OF PHYSICAL CHEMISTRY B · APRIL 2002

Impact Factor: 3.3 · DOI: 10.1021/jp025586l

3 AUTHORS, INCLUDING:

Vassiliki-Alexandra Glezakou
Pacific Northwest National Laboratory
43 PUBLICATIONS **515** CITATIONS
SEE PROFILE

Kyriakos Viras
National and Kapodistrian University of Athens
83 PUBLICATIONS **1,047** CITATIONS
SEE PROFILE

Low-Frequency Raman Spectroscopy of *n*-Alcohols. LAM Vibration and Crystal Structure

Maria Soutzidou, Vassiliki-Alexandra Glezakou, and Kyriakos Viras*

National and Kapodistrian University of Athens, Chemistry Department, Physical Chemistry Laboratory, Panepistimiopolis, Athens 157 71, Greece

Madeleine Helliwell, Andrew J. Masters, and Mark A. Vincent

Department of Chemistry, University of Manchester, Manchester M13 9PL, U.K.

Received: February 1, 2002

Low-frequency Raman spectra of even and odd *n*-alcohols have been recorded. The longitudinal acoustic modes (LAM) are described, and the effects of hydrogen-bonding, chain length, and temperature on the frequencies of these vibrations are discussed. The frequencies of the LAMs are interpreted in terms of the one-dimensional crystal model of Minoni and Zerbi and also ab initio calculations on isolated single chains. The low-frequency LAM-1 mode of the hydrogen-bonded dimer exhibited an odd−even effect, and to gain insight into this, the crystal structures of the C_{17} and C_{20} alcohols were determined by single-crystal X-ray diffractometry. $C_{17}H_{35}OH$ packs in the β form, with half the oxygen atoms trans and half gauche, with respect to the alkyl chains. $C_{20}H_{41}OH$ adopts an all trans conformation and the packing is in the γ form. The hydrogen-bonding interactions differ in the two structures. We therefore ascribe the odd−even effect in the LAM-1 frequencies to an odd−even effect in crystal structure.

1. Introduction

A number of chain length dependent bands have been observed in the low-frequency Raman spectra of crystalline *n*-alkanes,[1] as well as in other oligomers and semicrystalline polymers.[2] Among these bands, the one-node longitudinal acoustic mode (LAM-1) has been used for the determination of chain morphology in lamellar crystals of polymers.[2] For the *n*-alkanes, it has been shown by experiment that the LAM-1 frequency is approximately inversely proportional to the chain length.[3−6]

Within a degree of approximation, the frequencies of LAM-1 bands can be calculated by using the model of an isolated elastic rod with free ends.[3] The perturbation of the LAM-1 frequencies by end effects, such as interlayer forces and the inertial masses of end groups, has been investigated theoretically by modeling with a perturbed elastic rod[7,8] or a linear crystal,[9] while extra insight has been gained by calculation of normal modes.[2,10,11] Experimental studies of these effects based on end-modified *n*-alkanes have been reported by several authors.[12−19] Reports from our laboratories have encompassed not only high-modulus trans-planar *n*-alkanes and their derivatives[17−19] but also low-modulus helical oligo(oxyethylene)s.[20−22] We have shown that the LAM-1 frequencies of trans-planar alkyl chains are very sensitive to end-group mass and relatively insensitive to temperature, while the LAM-1 frequencies of helical oligo(oxyethylene) chains are most sensitive to interlayer force and are more temperature dependent.

The low-frequency Raman spectra of several *n*-alcohols, with chain lengths between C_{13} and C_{30}, were recorded in the present study. Low-frequency modes were assigned on the basis of the spectra of the *n*-alkanes and their mono- and disubstituted derivatives,[1,14−19] and on calculation of frequencies via linear crystal and ab initio procedures. The probability that crystal structure plays a role in determining the LAM-1 frequency was considered, and with this in mind, the crystal structures of the C_{17} and C_{20} alcohols were determined. There are several papers documenting X-ray crystal data on *n*-alcohols,[23−29] not all of which provide atomic coordinates. It is known that the higher ($>C_{12}$) even *n*-alcohols commonly crystallize in a form with the alkyl chains tilted from the end-group plane (γ form, monoclinic). Results for the odd alcohols are incomplete, but those available indicate that they crystallize in a form with the alkyl chains almost vertical to the end-group plane (β form, monoclinic but sometimes referred to as orthorhombic).[25,29] Our investigation covered this ground but was primarily focused on the nature and orientation of the hydrogen bonds in the crystal.

2. Experimental Section

2.1. Materials. The *n*-alcohols were obtained from various commercial sources. All the materials were used as received.

2.2. Raman Spectroscopy. Raman scattering at 90° to the incident beam was recorded by means of a Spex Ramalog spectrometer fitted with a 1403 double monochromator, and with a third (1442U) monochromator operated in scanning mode. The light source was a Coherent Innova 90 argon-ion laser operated at 514.5 nm and 300 mW. Typical operating conditions for low-frequency spectra (<250 cm^{-1}) were bandwidth 1.0 cm^{-1}, scanning increment 0.05 cm^{-1}, and integration time 6 s. For high-frequency spectra (<1800 cm^{-1}) the conditions were bandwidth 3.0 cm^{-1}, scanning increment 0.5 cm^{-1}, and integration time 4 s. On occasion, for very low frequencies, the conditions were bandwidth 0.8 cm^{-1}, scanning increment 0.01 cm^{-1}, and integration time 8 s. The frequency scale was calibrated by reference to the 9.6 and 14.9 cm^{-1} bands in the low-frequency spectrum of L-cystine.

Samples were enclosed in capillary tubes and held at a constant temperature at 293 ± 1 K. A Harney-Miller cell (Spex Industries) was used for measurements over the range 173−

10.1021/jp025586l CCC: $22.00
Published on Web 04/03/2002

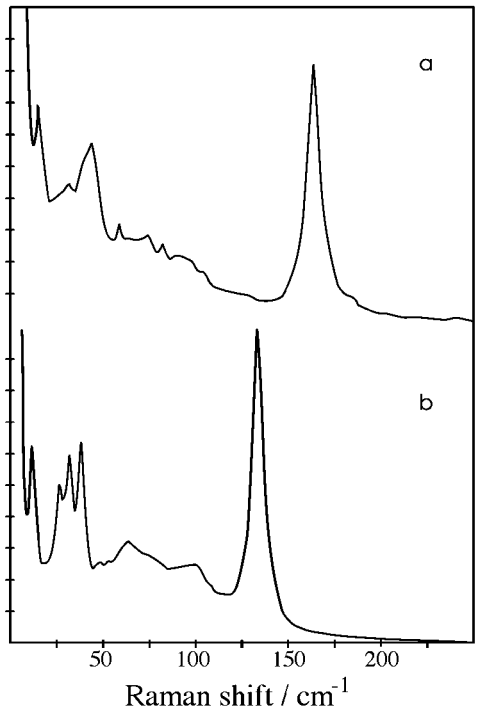

Figure 1. Low-frequency Raman spectra (intensity versus Raman shift) of crystalline even *n*-alcohols at 293 K: (a) $C_{14}H_{29}OH$; (b) $C_{18}H_{37}OH$.

293 K. At the lowest temperature investigated, 77 K, the sample was held to ±0.5 K within the vacuum chamber of an Oxford Instruments Ltd. Model CF104 cryostat plus Model CF5244 temperature control unit. In the experiments, the intensity of a suitable Raman band was observed over a period of time to ensure equilibrium of the sample at a given temperature. Generally, high-frequency spectra were recorded before and immediately after the low-frequency spectra, to confirm that samples were unchanged by exposure to the laser beam. Spectra were recorded several times, and band frequencies were obtained as averages of many observations. The uncertainty in average frequency was estimated to be ±0.5 cm^{-1} for the low-frequency bands and ±1 cm^{-1} for the high-frequency bands.

2.3. X-ray Diffraction. Samples of the C_{17} and C_{20} alcohols were recrystallized by very slow evaporation of dichloromethane/hexane solutions, over approximately one month, which in each case yielded weakly diffracting, thin platelike crystals. Suitable crystals for X-ray structure analysis were then mounted on glass fibers, and data collection was carried out on a high-intensity Cu Kα rotating anode Rigaku AFC-5R diffractometer at room temperature.

3. Raman Spectroscopy and the LAM Bands

Selected low-frequency spectra (5−250 cm^{-1}) are shown in Figures 1 and 2, and band frequencies are listed in Table 1. Selected frequencies are assigned as discussed below.

Assignments of LAM bands was aided by application of the linear crystal model of Minoni and Zerbi.[9] In their bilayer crystals, the alcohols interact through their hydroxyl groups forming hydrogen-bonded dimers which are themselves subject to van der Waals end forces. Modeling the system as a one-dimensional crystal with chain groups represented by point masses leads to the representation shown in Figure 3a. The CH_2 chain groups and the CH_3 and CH_2OH end groups are represented by point masses m_c, m_e, and m_h respectively, and

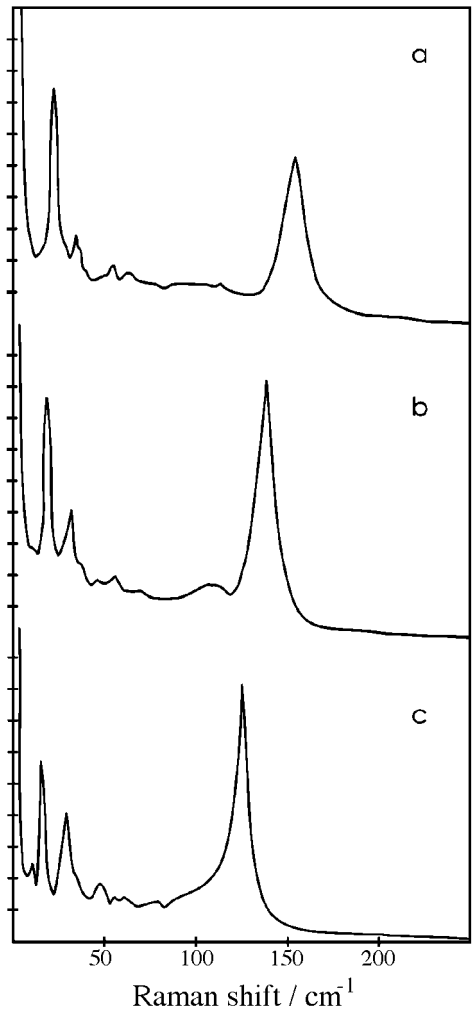

Figure 2. Low-frequency Raman spectra (intensity versus Raman shift) of crystalline odd *n*-alcohols at 293 K: (a) $C_{15}H_{31}OH$; (b) $C_{17}H_{35}OH$; (c) $C_{19}H_{39}OH$.

the interactions between them are represented by force constants f_c, f_e, and f_h, respectively.

Equations for infinite one-dimensional crystals with symmetrical unimeric or dimeric repeat units have been derived by Minoni and Zerbi[9] and applied to the case of *n*-octadecanol.[15] In related work we adopted Zerbi's approach in interpreting the Raman spectra of oligo(oxyethylene)s with hydroxy, methyl, or *n*-alkyl end groups, including treating unsymmetrical cases.[20−22] The equations used in this work for a crystal in which the repeat unit is an H-bonded dimer have been set out previously.[20]

The notation to be used requires definition. Wave profiles calculated for the first two longitudinal modes of the H-bonded dimer (details given below) are shown in Figure 3b. The numbers of nodes per dimeric repeat unit are 2 for mode (i) and 4 for mode (ii); i.e., they are LAM-2 and LAM-4 of the crystal repeat unit. Discounting the node centered in the van der Waals bond allows the familiar LAM-1 and LAM-3 nomenclature to be used for modes (i) and (ii) of the dimer. Discounting the node-centered in the H-bond allows mode (ii) to be denoted LAM-1 of the alcohol (unimer), i.e., parallel to the notation for *n*-alkanes. However, in this report the LAM-1/LAM-3 notation is preferred.

3.1. LAM-3. Assignment of bands to LAM-3 of the H-bonded dimer was apparent on inspection of the spectra (see Figures 1 and 2): i.e., the intense bands at frequencies in the range 85−180 cm-[1]. The observed LAM-3 frequencies (see Table 1 for

TABLE 1: Low-Frequency Raman Bands of Crystalline H-Bonded Dimers of *n*-Alcohols at 293 K

n	LAM-1 cm^{-1}	LAM-3 cm^{-1}	PLAM-1 cm^{-1}	OPB-1 cm^{-1}	IPB cm^{-1}	other bands/cm^{-1}
13	43.6	178.5	142	30.2	31.9	12.6, 68.7, 120.0
14	46.4	168.0	130	28.4	33.3	17.0, 60.3
15	38.7	158.0	115	26.2	29.7	10.7, 44.2, 58.3, 68.1
17	35.7	142.1		23.2	27.7	9.5, 41.7, 51.5, 60.8, 73.0, 108
18	39.4	135.5		27.9	32.2	13.5, 50.4, 64.1, 76.4, 104
19	33.5	129.0		20.7	22.4	8.1, 38.1, 52.2, 58.9, 64.4, 96.8
20	37.9	124.0		26.0	30.3	12.0, 41.6, 61.4, 81.2, 104
22	36.6	114.6		24.1	27.4	11.8, 43.7, 60.4, 86.1, 98.5
26	31.4	100.0		21.2	21.4	11.6, 37.6, 51.0, 70.3, 87.6
30	29.6	87.6		20.0	20.0	13.0, 44.6, 67.3, 78.2

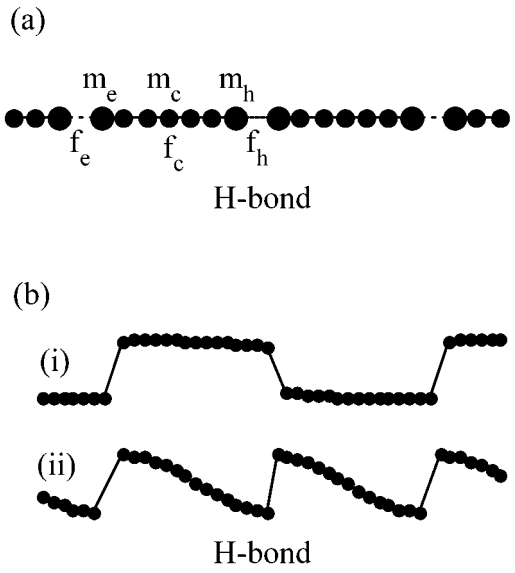

Figure 3. H-bonded dimers of an *n*-alcohol in a one-dimensional crystal. (a) The model: symbols *m* and *f* indicate masses and force constants; subscripts c, e, and h indicate methylene chain groups, methyl end groups, and methylol end groups, respectively. (b) Wave profiles: (i) LAM-1 and (ii) LAM-3 of the dimer.

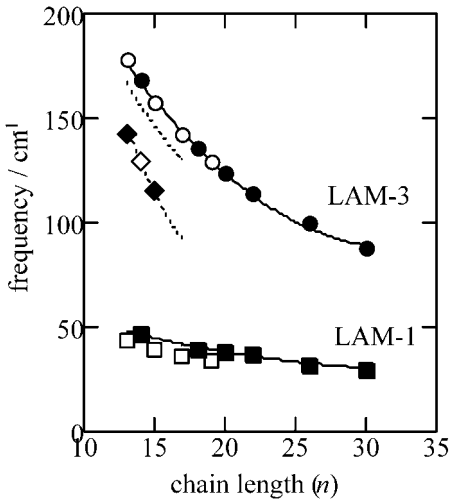

Figure 4. Effect of chain length on the LAM frequencies of crystalline even *n*-alcohols (filled symbols) and crystalline odd *n*-alcohols (unfilled symbols) at 293 K. The squares refer to LAM-1 and the circles to LAM-3 of the hydrogen-bonded dimer, as indicated. Data points for the pseudo-LAM-3 are indicated by diamonds. The solid curves were calculated using the linear crystal model[9,20] with $f_c = 460$ N m^{-1}, $f_h = 12$ N m^{-1}, and $f_e = 3$ N m^{-1}. The dotted curves were calculated using the ab initio method (see text).

values) are plotted against chain length (C_n) in Figure 4. Values of the LAM-3 frequency were calculated using the linear crystal model with $m_c = 2.33 \times 10^{-26}$ kg, $m_e = 2.50 \times 10^{-26}$ kg, $m_h = 5.15 \times 10^{-26}$ kg, $f_c = 460$ N m^{-1}, $f_e = 3$ N m^{-1}, and $f_h = 12$ N m^{-1}. As can be seen in Figure 4, these parameters gave a satisfactory fit to the observed frequencies. The values of f_e and f_h are the same as those used previously for oligo(oxyethylene)s[20,21] and are similar to those used previously for alkanediols and monobromides[17−19] (i.e., $f_h = 15$ N m^{-1} and $f_e = 5$ N m^{-1}, respectively). The value of f_c is higher than that (420 N m^{-1}) used previously to fit the LAM frequencies of *n*-alkanes and their mono- and disubstituted derivatives.[17−19] Calculations based on $f_c = 420$ N m^{-1} with a variety of values of f_e and f_h were carried out in the present study, but a good fit to the values of LAM-3 of the dimer could not be forced. Minoni et al. in their study of *n*-octadecanol adopted a slightly different approach, but effectively used values of $f_c = 520$ N m^{-1}, $f_h = 18$ N m^{-1}, and $f_e = 0$.[9,15]

3.2. LAM-1 and Other Low-Frequency Bands. Direct assignment to the LAM-1 band of the dimer was not possible, since these bands were in the same frequency range of the spectra as the bending modes: i.e., 25−47 cm^{-1} (see Figures 1 and 2). Calculations based on the linear crystal model, with exactly the same parameters as used for fitting the values of LAM-3, pointed to the highest frequency bands of the groups as LAM-1. With this assignment the LAM-1 frequencies show a pronounced even−odd effect, the data points for the odd *n*-alcohols falling some 6 cm^{-1} below the calculated curve: see Figure 4.

In studies of the low-frequency Raman spectra of *n*-alkanes[1,3] and disubstituted *n*-alkanes,[17,18] bands in the region 10−50 cm^{-1} have been assigned to in-plane and out-of-plane whole-chain bending modes, IPB-1 and OPB-1. These two bands are resolved in the spectra of the shorter *n*-alkanes (e.g., $n < C_{16}$),[1] but less readily so at longer chain lengths. The lower frequency bands in the range 25−35 cm^{-1} in the spectra of the *n*-alcohols (see Figures 1 and 2) are analogously assigned; see Table 1.

3.3. Ab Initio Calculations. Recent ab initio calculations by Meier[11] on disubstituted *n*-alkanes have shown that the LAM-1 mode shows an odd−even effect even for an isolated chain, provided the head and tail groups are heavy enough. We therefore used the Gaussian 94 suite of programs[30] to conduct ab initio calculations on the C_{13}−C_{17} alcohols at the Hartree−Fock level, using a 3-21g basis set.[31] These calculations were for a single isolated chain, not for a hydrogen-bonded dimer. The structures were optimized at this level of theory and the frequencies of the all normal modes were calculated. Comparison of the LAM mode with the experimental results for LAM-3 (see Figure 4) shows that the calculated values (dotted curve) fall some 10 cm^{-1} below the experimental values, undoubtedly

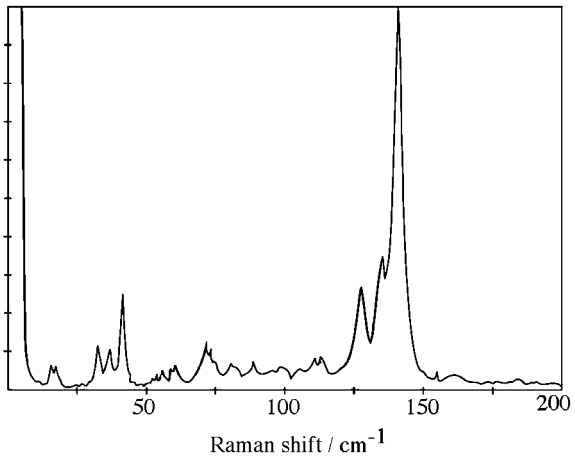

Figure 5. Low-frequency Raman spectrum (intensity versus Raman shift) of crystalline $C_{18}H_{37}OH$ at 77 K.

because of neglect of the head-to-head hydrogen bonding that occurs in the real system.

For the *n*-alkanes, there is a mode with a somewhat lower frequency than the LAM mode in which the atomic motions are rather similar to those found in the true LAM mode, but with some extra transverse components. This mode is also present in bromoalkanes, as noted by Chang and Krimm[16] and by Meier.[11] In the notation of Olf and Fanconi this pseudo-LAM (PLAM) mode is designated as an early member of the band series of the longitudinal acoustical branch.[1] As seen in Figures 1 and 2, bands in this region are very weak in the spectra of the *n*-alcohols, as is also the case for the bromoalkanes.[16] Calculated values for this mode are shown as the lower dotted curve in Figure 4, where they are seen to correspond well to the experimental frequencies of bands detected in the spectra of the shorter chains. On this basis, those bands are designated PLAM-3 in Table 1. As there will be more rocking and less direct stretching of the hydrogen bond in this mode as compared to the LAM-3 mode, one might expect the influence of the hydrogen bonding to be less.

To investigate the odd−even effect of the observed LAM-1 mode of the crystal, it would be necessary to model the modes of an alcohol dimer. Unfortunately, at the level of theory used, the optimized geometry for an alcohol dimer is far from linear and the calculated modes of vibration have little relevance to the modes of vibration in the crystal. However, we note that heavy end groups are needed for an odd−even effect to become noticeable in the LAM vibration of an isolated chain, and a hydroxide group is too light. This was pointed out by Meier[11] and is confirmed by our own calculations using the Gaussian 94 programs.

3.4. Effect of Temperature. Low-frequency spectra were recorded for the C_{13} and C_{18} alcohols at temperatures in the range 173−293 K. That of $C_{18}H_{37}OH$ was additionally recorded with the sample at 77 K. This spectrum is shown in Figure 5: compared with those in the spectrum obtained with the sample at 293 K (see Figure 1), the minor bands are more clearly resolved. The effect of temperature on the LAM-1 and LAM-3 frequencies of the dimer is shown in Figure 6. Averaged over the temperature interval, the temperature dependence is approximately -0.030 cm^{-1} K^{-1} in each case. Closer analysis indicates curvature, as might be expected for LAM modes. Rabolt[14] has reported a similar value, -0.032 cm^{-1} K^{-1} for the dimer LAM-3 frequency of the C_{18} alcohol. These values can be compared with the much smaller value, -0.006 cm^{-1} K^{-1},

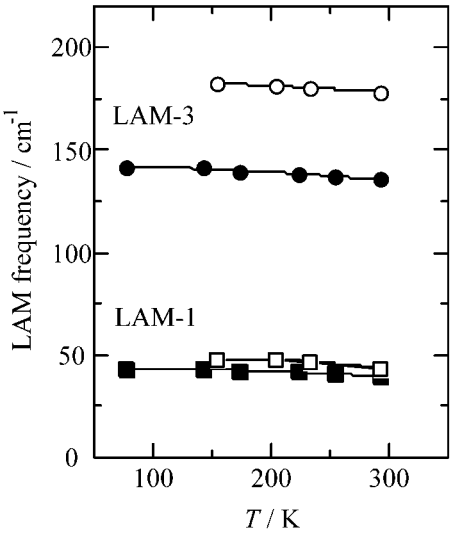

Figure 6. Temperature dependence of the LAM-1 and LAM-3 frequencies of H-bonded dimers of *n*-alcohols. Unfilled symbols denote $C_{13}H_{27}OH$; filled symbols denote $C_{18}H_{37}OH$. The curves are least-squares quadratic fits to the data points.

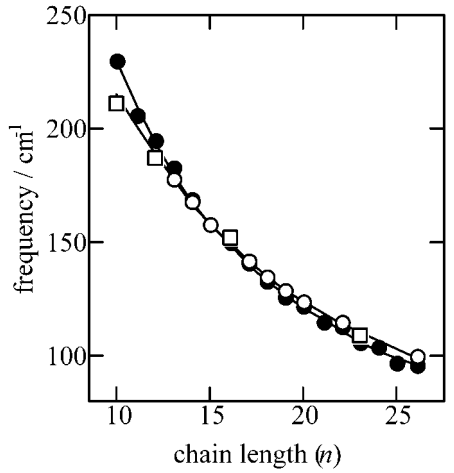

Figure 7. Effect of chain length on the LAM frequencies of crystalline chain molecules at 293 K: (●) *n*-alkanes (LAM-1); (○) *n*-alcohols (dimer LAM-3); (□) α,*ω*-alkanediols (equivalent dimer LAM-3). The curves are calculated using the linear crystal model.

obtained for the LAM-1 frequency of crystalline octadecane.[14] The larger effect of temperature on the LAM frequencies of the alcohol is attributable to the contraction of the lattice shortening the hydrogen bond, so increasing LAM-1 and inducing an increase in strength of the interaction that perturbs the LAM-3 frequency.

3.5. Comparison with *n*-Alkanes. In Figure 7 LAM frequencies obtained in the present work on the *n*-alcohols (i.e., LAM-3 frequencies of the dimers) are compared with published LAM-1 frequencies of *n*-alkanes[1] and alkanediols.[17,18] The near correspondence of the data points across the frequency range results from opposing effects: a decrease in frequency caused by the heavier end group(s) of the mono-ols and diols compared to the alkanes (i.e., CH_2OH compared with CH_3) being compensated by an increase in frequency caused by the end forces resulting from hydrogen bonding. Detailed inspection of Figure 7 shows practically complete compensation of the two effects at $n = 15$, with the effect of end forces being favored at $n > 15$ (i.e., at high frequencies) and the effect of end mass being favored at $n < 15$ (i.e., at low frequencies). This effect

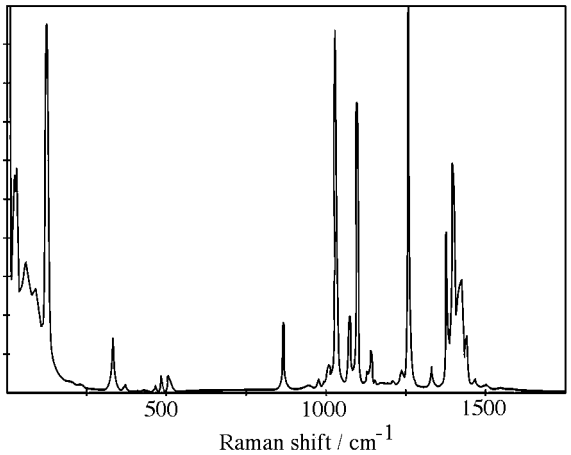

Figure 8. Raman spectrum (intensity versus Raman shift, 100−1800 cm^{-1}) of crystalline $C_{18}H_{37}OH$ at 293 K.

TABLE 2: Unit Cell Parameters for *n*-Alcohols

	$C_{17}H_{35}OH$	$C_{20}H_{41}OH$
crystal system	monoclinic	monoclinic
space group	*P*21/*c*	*C*2/*c*
a/Å	5.046	91.070
b/Å	7.355	4.943
c/Å	95.72	8.933
β/deg	97.35	92.964

of chain length is in keeping with physical intuition and is as predicted by calculation based on the linear crystal model.

4. Crystal Structures by X-ray Diffraction

The evidence presented in section 3 supports the view that the odd−even effect in the LAM-1 mode is due to a difference in crystal structure rather than being a property of the single chain. High-frequency Raman spectra can give important information on crystal structure but, unfortunately, not in the present case as the spectra were very similar for all the alcohols studied. In the high-frequency spectrum of the C_{18} alcohol, shown in Figure 8, the splitting of the methylene-bending mode near 1440 cm^{-1} has been attributed to a crystal field effect, but the same splitting is associated with both odd and even alcohols.[32]

To investigate the even−odd effect as thoroughly as possible, the crystal structures of C_{17} and C_{20} alcohols were studied using X-ray diffraction. The melting points of these two alcohols were high enough to allow their crystallization from dilute solution at room temperature, while their long spacings did not take them outside the range of the analysis. The unit cell parameters obtained are listed in Table 2. The data collection and refinement parameters are listed in Tables A1 and A2.

4.1. $C_{17}H_{35}OH$. In the case of *n*-$C_{17}H_{35}OH$, the *c* axis was so long that the peaks tended to overlap, leading to inaccuracies in background and intensity measurements. To reduce this problem, vertical and horizontal slits were used to lower the effective size of the detector aperture. Also, the Lehmann-Larsen algorithm[33] was employed for profile fitting, to improve the accuracy of intensity determinations. The crystal structure was solved by direct methods (SIR92),[34] and refinement was carried out on F^2 using SHELXL97.[35] The non-hydrogen atoms were refined anisotropically. Methylene hydrogen atoms were included in constrained positions using the riding method. Methyl hydrogen atoms were also included in constrained positions, using as a starting point, the positions of maximum electron density. Attempts made to locate the hydroxyl hydrogen atoms by difference Fourier techniques were unsuccessful, so instead they were included in constrained positions, so as to maximize the hydrogen-bonding interactions.

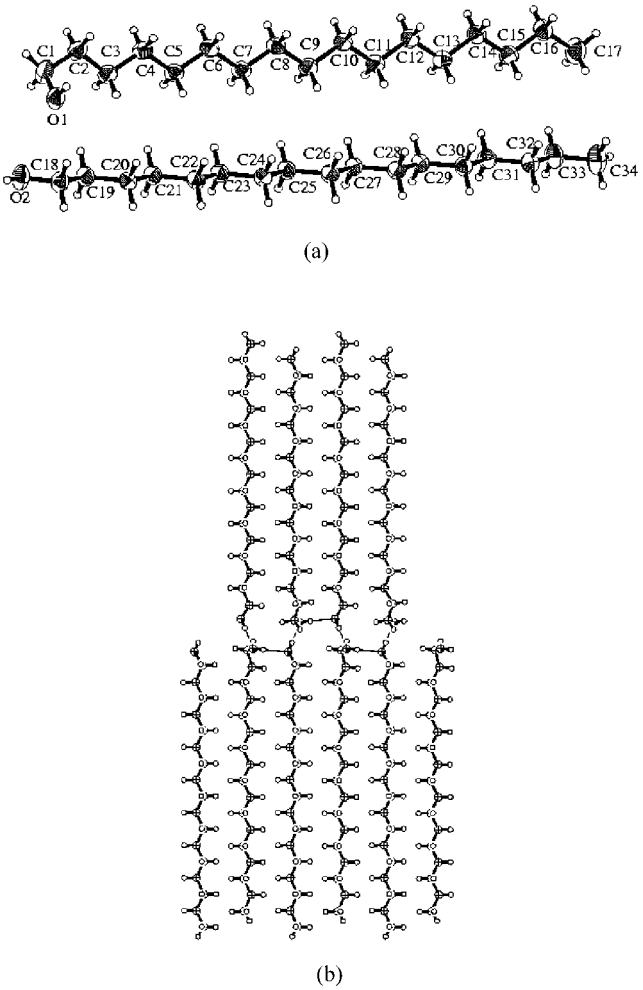

Figure 9. (a) Asymmetric unit in crystalline $C_{17}H_{35}OH$. (b) Packing of crystalline $C_{17}H_{35}OH$ viewed down the *a*-axis.

In the crystal the asymmetric unit contains two molecules, one of which has the oxygen atom in the gauche conformation (O1 in Figure 9a), while the other molecule adopts a trans conformation (O2 in Figure 9a). The packing arrangement is the monoclinic *β* form with the hydroxyl groups arranged in planes, and the alkyl chains vertical to the layer planes (Figure 9b). There are two forms of hydrogen-bonding interactions, one within the layer with an oxygen−oxygen distance of 2.790 Å, and the other between the layers with an oxygen−oxygen distance of 2.708 Å.

4.2. $C_{20}H_{41}OH$. *n*-$C_{20}H_{41}OH$ also has a long axis but, since the cell is C-centered monoclinic, data could be collected using the standard $\omega-2\theta$ scan mode. The structure was solved using MITHRIL90[36] and refined using SHELXL97.[35] All non-hydrogen atoms were refined anisotropically, and hydrogen atoms bonded to carbon were included as for *n*-$C_{17}H_{35}OH$. Again, the hydroxyl hydrogen atoms could not be found by difference Fourier techniques, and there are two positions for each which maximize the hydrogen-bonding interactions. Therefore, these atoms were included disordered over two sites, each at an occupancy of 0.5.

For this crystal, the unit cell dimensions, the space group symmetry, and the packing arrangement are similar to those

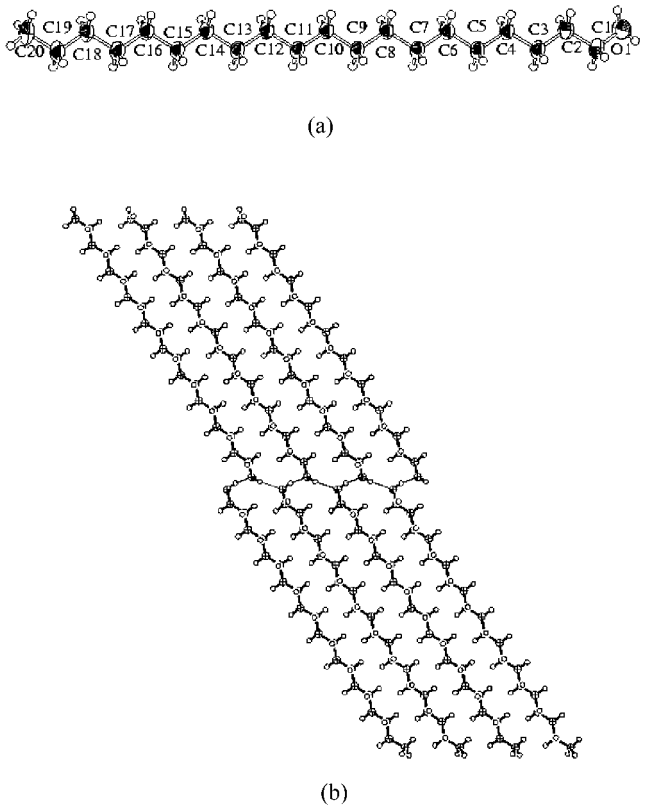

Figure 10. (a) Asymmetric unit in crystalline $C_{20}H_{41}OH$ showing disordered hydroxyl protons. (b) Packing of crystalline $C_{20}H_{41}OH$ viewed down the *b*-axis. For clarity the disordered protons are omitted from (b).

reported for other even *n*-alcohols, allowing for the differing lengths of the alkyl chains.[24−27,29] The asymmetric unit of the C_{20} crystal consists of one molecule that adopts the trans conformation (Figure 10a). The packing arrangement is the monoclinic γ form, with the molecules tilted with respect to the layers formed by the hydroxyl groups (Figure 10b). Hydroxyl hydrogen atoms can be placed in two possible positions so as to maximize the hydrogen-bonding interactions, with oxygen−oxygen contacts of 2.713 and 2.680 Å, respectively. Both options must be present in the crystal, although not within the same hydrogen-bonded chain.

The implication of the structural information for the LAM-1 vibration of the hydrogen-bonded dimer is clear. In the crystal of the C_{20} alcohol (Figure 10) the hydrogen bond connects two alcohols that are essentially collinear and the LAM-1 mode directly stretches the hydrogen bond. However, in the crystal of the C_{17} alcohol (Figure 9) half the chains have their oxygen in a gauche conformation and the hydrogen bond connects alcohols that are in different layer planes. This hydrogen bond is not collinear with the chain backbones and the LAM-1 mode will bend the hydrogen bond rather than directly stretch it. If we assume that all the even alcohols investigated by Raman spectroscopy form only collinear dimers in the crystal but that the odd alcohols dimers do not, then in terms of the Minoni−Zerbi model the effective spring constant of the hydrogen bond should be smaller for the odd alcohols than for the even ones. This would mean that the LAM-1 frequencies of the odd alcohols would lie on a curve beneath that formed from the chain frequencies of the even alcohols. Experimentally this is what is observed, as shown in Figure 4. We therefore ascribe the odd−even effect in LAM-1 to differences in crystal structure.

TABLE A1: Crystal Data

	C_{17}	C_{20}
formula	$C_{17}H_{36}O$	$C_{20}H_{42}O$
M_r	256.46	298.54
a (Å)	5.046(2)	91.070(12)
b (Å)	7.355(6)	4.9427(12)
c (Å)	95.72(4)	8.993(3)
β (deg)	97.35(4)	92.964(17)
V (Å^3)	3523(4)	4042.5(18)
crystal system	monoclinic	monoclinic
space group	$P2_1/c$	$C2/c$
Z	8	8
D_c (Mg m^{-3})	0.967	0.981
μ (mm^{-1})	0.421	0.421
crystal size (mm)	1.00 × 0.5 × 0.02	1.00 × 0.5 × 0.02
radiation	Cu Kα	Cu Kα
wavelength (Å)	1.5418	1.5418
diffractometer	Rigaku AFC-5R	Rigaku AFC-5R
scan type	ω	$\omega-2\theta$
θ_{max} (deg)	78.52	78.32
index range	$h = -6 \rightarrow 6$ $k = -7 \rightarrow 9$ $l = -95 \rightarrow 121$	$h = -97 \rightarrow 114$ $k = -6 \rightarrow 6$ $l = -10 \rightarrow 10$
no. of measd, ind reflns	7182, 7141	9735, 4108
corrections applied	Lorentz polarization	Lorentz polarization absorption based on three ψ scans;[37] $T_{max} = 1.00$, $T_{min} = 0.877$
R_{int}	0.0433	0.1657
reflns with $I > 2(\sigma)$	2205	1457
refinement on F^2		
$R(F)$, $wR(F^2)$	0.0976, 0.3892	0.1003, 0.4247
S	0.964	1.119
Δ/σ_{max}	0.002	0.000
max, min peaks on final diff maps (e Å^3)	0.381, −0.421	0.328, −0.338
no. of parameters	327	190
data collection and graphics software	ref 38	ref 38

TABLE A2: Hydrogen Bonds

	OH bond length (Å)	H···A dist (Å)	O−H···A angle (deg)	O···A dist (Å)	A [symm element]
			$C_{17}H_{35}OH$		
O1−H1	0.820	1.974	173.66	2.790	O2 [$x, y+1, z$]
O2−H2	0.820	1.893	173.24	2.708	O1 [$-x+2, y-{}^1/_2, -z+{}^1/_2$]
			$C_{20}H_{41}OH$		
O1−H11	0.820	1.904	168.80	2.713	O1 [$-x, -y+2, -z$]
O1−H12	0.820	1.876	166.32	2.680	O1 [$-x, y, -z+{}^1/_2$]

Acknowledgment. We are pleased to acknowledge practical help from Mr P. Kobryn, and financial assistance from the Royal Society of Chemistry Journals Grants for International Authors. We thank Dr. R. J. Meier for informing us of his calculations prior to publication. Finally, we are grateful to Dr. C. Booth for helpful advice.

References and Notes

(1) Olf, H. G.; Fanconi, B. *J. Chem. Phys.* **1973**, *59*, 534.
(2) Rabolt, J. F. *CRC Crit. Rev. Solid State Mater. Sci.* **1977**, *12*, 165.
(3) Mizushima, S.; Shimanouchi, T. *J. Am. Chem. Soc.* **1949**, *71*, 1320.
(4) Schaufele, R. F.; Shimanouchi, T. *J. Chem. Phys.* **1967**, *47*, 3605.
(5) Ungar, G. In *Interpretation of Fundamental Polymer Science and Technology*; Lemstra, P. J.; Kleintjens, L. A., Eds; Elsevier Applied Science: London, 1988; Vol. 2, p 364.
(6) Snyder, R. G.; Strauss, H. L.; Alamo, R.; Mandelkern, L. *J. Chem. Phys.* **1994**, *100*, 5422.
(7) Strobl, G. R.; Eckel, R. *J. Polym. Sci., Polym. Phys. Ed.* **1976**, *14*, 913.
(8) Hsu, S. L.; Krimm, S. *J. Appl. Phys.* **1976**, *47*, 4265.

(9) Minoni, G.; Zerbi, G. *J. Phys. Chem*. **1982**, *86*, 4791.
(10) Chang, C.; Krimm, S. *J. Appl. Phys.* **1983**, *58*, 5526.
(11) Meier, R. J. *Vibr. Spectrosc.* **2000**, *24*, 165.
(12) Fanconi, B.; Chissman, J. *J. Polym. Sci., Polym. Lett. Ed*. **1975**, *13*, 421.
(13) Nomura, H.; Koda, S.; Kawalzumi, F.; Miyahara, Y. *J. Phys. Chem*. **1977**, *81*, 226.
(14) Rabolt, J. F. *J. Polym. Sci., Polym. Phys. Ed*. **1979**, *17*, 1457.
(15) Minoni, G.; Zerbi, G.; Rabolt, J. F. *J. Chem. Phys*. **1984**, *81*, 4781.
(16) Chang, C.; Krimm, S. *J. Polym. Sci., Part B, Polym. Phys.* **1986**, *24*, 1373.
(17) Viras, K.; Viras, F.; Campbell, C.; King, T. A.; Booth, C. *J. Phys. Chem*. **1989**, *93*, 3479.
(18) Viras, F.; Viras, K.; Campbell, C.; King, T. A.; Booth, C. *J. Polym. Sci., Polym. Phys. Ed*. **1991**, *29*, 1467.
(19) Soutzidou, M.; Masters, A. J.; Viras, K.; Booth, C. *Phys. Chem. Chem. Phys.* **1999**, *1*, 415.
(20) Campbell, C.; Viras, K.; Masters, A. J.; Craven, J. R.; Zhang, H.; Yeates, S. G.; Booth, C. *J. Phys. Chem*. **1991**, *95*, 4647.
(21) Craven, J. R.; Viras, K.; Masters, A. J.; Booth, C. *J. Chem. Soc., Faraday Trans.* **1991**, *87*, 3677.
(22) Campbell, C.; Viras, K.; Booth, C. *J. Polym. Sci., Polym. Phys. Ed*. **1991**, *29*, 1613.
(23) Tanaka, K.; Seto, T.; Hayashida, T. *Bull. Inst. Chem. Res. Kyoto University* **1957**, *35*, 123.
(24) Abrahamsson, S.; Larsson, G.; von Sydow, E. *Acta Crystallogr*. **1960**, *13*, 770.
(25) Tasumi, M.; Shimanouchi, T.; Watanabe, A.; Goto, R. *Spectrochim. Acta* **1964**, *20*, 629.
(26) Precht, D. *Fette Seifen* **1976**, *78*, 189.
(27) Fujimoto, T.; Yamamoto, T.; Hara, T. *Rep. Prog. Polym. Phys. Jpn.* **1985**, *28*, 163.
(28) Yamamoto, T.; Nozaki, K.; Hara, T. *J. Chem. Phys.* **1990**, *92*, 631.
(29) Wang, J.-L.; Leveiller, F.; Jacquemain, D.; Kjaer, K.; Als-Nielsen, J.; Lahav, M.; Leiserowitz, L. *J. Am. Chem. Soc.* **1994**, *116*, 1192.
(30) Frisch, M. J.; Trucks, G. W.; Schlegel, H. B.; Gill, P. M. W.; Johnson, B. G.; Robb, M. A.; Cheeseman, J. R.; Keith, T. A.; Petersson, G. A.; Montgomery, J. A.; Raghavachari, K.; Al-Laham, M. A.; Zakrzewski, V. G.; Ortiz, J. V.; Foresman, J. B.; Cioslowski, J.; Stefanov, B. B.; Nanayakkara, A.; Challacombe, M.; Peng, C. Y.; Ayala, P. Y.; Chen, W.; Wong, M. W.; Andres, J. L.; Replogle, E. S.; Gomperts, R.; Martin, R. L.; Fox, D. J.; Binkley, J. S.; Defrees, D. J.; Baker, J.; Stewart, J. P.; Head-Gordon, M.; Gonzalez, C.; Pople, J. A. *Gaussian 94*, Revision A1; Gaussian Inc.: Pittsburgh, PA, 1995.
(31) Binkley, J. S.; Pople, J. A.; Hehre, W. J. *J. Am. Chem. Soc*. **1980**, *102*, 939.
(32) Boerio, F. J.; Koenig, J. L. *J. Chem. Phys.* **1970**, *52*, 3425.
(33) Lehmann, M. S.; Larsen, F. K. *Acta Crystallogr*. **1974**, *A30*, 580.
(34) Altomore, A.; Cascarano, M.; Giacovazzo, C.; Guadliardi, A. *SIR92*, *J. Appl. Crystallogr*. **1993**, *26*, 343.
(35) Sheldrick G. M. *SHELXL97, Program for Automatic Structure Refinement*; University of Gottingen: Gottingen, Germany, 1997.
(36) Gilmore, C. J. *MITHRIL, An Integrated Direct Methods Computer Program*; University of Glasgow: Glasgow, Scotland, 1990.
(37) North, A. C. T.; Phillips, D. C.; Mathews, F. S. *Acta Crystallogr*. **1968**, *A24*, 351.
(38) Molecular Structure Corporation. 1995. teXsan. Single-Crystal Structure Analysis Software. Version 1.7. MSC, 3200 Research Forest Drive, The Woodlands, TX 77381.